Initial ciliary assembly in *Chlamydomonas* requires Arp2/3 complex-dependent endocytosis

Brae M Bigge[1,2], Nicholas E Rosenthal[1,2], Prachee Avasthi[1,2]

[1]Biochemistry and Cell Biology Department, Geisel School of Medicine at Dartmouth College, Hanover, New Hampshire
[2]Anatomy and Cell Biology Department, University of Kansas Medical Center, Kansas City, Kansas

ABSTRACT

Ciliary assembly, trafficking, and regulation are dependent on microtubules, but the mechanisms of ciliary assembly also require the actin cytoskeleton. Here, we dissect subcellular roles of actin in ciliogenesis by focusing on actin networks nucleated by the Arp2/3 complex in the powerful ciliary model, *Chlamydomonas*. We find the Arp2/3 complex is required for the initial stages of ciliary assembly when protein and membrane are in high demand, but cannot yet be supplied from the Golgi complex. We provide evidence for Arp2/3 complex-dependent clathrin-mediated endocytosis of ciliary proteins, an increase in endocytic activity upon induction of ciliary growth, and relocalization of plasma membrane proteins to newly formed cilia. Our data support a new model of ciliary protein and membrane trafficking during early ciliogenesis whereby proteins previously targeted to the plasma membrane are reclaimed by Arp2/3 complex-dependent clathrin-mediated endocytosis for initial ciliary assembly.

INTRODUCTION

The cilium of the unicellular, green alga *Chlamydomonas reinhardtii* has long been used as a model due to its structural and mechanistic conservation relative to the cilia of mammalian cells. Cilia consist primarily of microtubules that extend from the surface of the cell and are ensheathed in plasma membrane. Their assembly relies on microtubule dynamics and trafficking of protein and membrane (Nachury, Seeley, and Jin 2010), as well as intraflagellar transport (IFT), a motor-based transport system that moves tubulin and other cargo from the base of the cilium to the tip and back again (Pedersen and Rosenbaum 2008).

Although cilia are composed of microtubules and depend on them for assembly, the mechanisms governing ciliary maintenance and assembly extend to other cytoskeletal components, namely actin. In fact, the microtubule organizing center of the cell, the centrosome, from which cilia are nucleated has been found to function as an actin organizer (Farina et al. 2016; Inoue et al. 2019). In mammalian cells, cortical actin disruption results in increased ciliary length and percentage of ciliated cells (Kim et al. 2010; Park et al. 2008). Further, in mammalian cells, when ciliogenesis is triggered by serum starvation, preciliary vesicles are trafficked to the centriole where they fuse to form a ciliary vesicle around the budding cilium. In the intracellular pathway of ciliogenesis, it has been shown that when Arp2/3 complex-branched actin is lost, depletion of preciliary vesicles at the centriole occurs due to problems with vesicle fusion, suggesting a role for branched actin in intracellular ciliogenesis (Wu, Chen, and Tang 2018). Further, actin itself has even been found within cilia, suggesting that actin is a key protein involved in ciliary maintenance and assembly (Kiesel et al. 2020).

Chlamydomonas cells are ideal for tackling the question of actin-dependent ciliary trafficking due to their lack of a cortical actin network and their ability to undergo consistent and robust ciliogenesis without requiring serum starvation. In *Chlamydomonas*, disruption of actin networks with Cytochalasin D (CytoD) resulted in shorter steady-state cilia (W. L. Dentler and Adams 1992) and disruption with Latrunculin B (LatB), which sequesters monomers leading to eventual filament depolymerization, resulted in shortened cilia and impaired regeneration (Avasthi et al. 2014; Jack et al. 2019). *Chlamydomonas* actin networks are required for accumulation of IFT machinery at the base of cilia and for entry of IFT material into cilia (Avasthi et al. 2014), as well as for trafficking of post-Golgi vesicles to cilia, the synthesis of ciliary proteins, and the organization of the gating region at the base of cilia (Jack et al. 2019). Many key advances in our understanding of the relationship between cilia and actin have been discovered using *Chlamydomonas*, which is proving to be a useful model for studying the actin cytoskeleton and its ciliary functions.

The actin cytoskeleton of *Chlamydomonas* contains two actin genes: *IDA5*, a conventional actin with 91% sequence identity to human β-actin; and *NAP1*, a divergent actin that shares only 63% of its sequence with human β-actin (Hirono et al. 2003; Kato-Minoura et al. 1998). We consider NAP1 to be an actin-like protein as opposed to an actin related protein (ARP) because it has a higher sequency identity to actin than to conventional ARPs, and because it is able to functionally compensate for the conventional filamentous actin (Jack et al. 2019; M. Onishi et al. 2018; M. Onishi, Pringle, and Cross 2016; Masayuki Onishi et al. 2019). Under normal, vegetative conditions, the conventional IDA5 is the primary actin expressed, but when cells are treated with LatB, the LatB-insensitive NAP1 is upregulated (M. Onishi et al. 2018; M. Onishi, Pringle, and Cross 2016; Hirono et al. 2003). This separability of the two actins has led to the discovery that they can compensate for each other in ciliary maintenance and assembly (Jack et al. 2019). Studies of the role of actin in ciliary assembly have used global disruption by knocking out either one of the filamentous actins or acutely knocking out both, yet actin networks have diverse compositions and topologies that lead to specific subfunctions within cells.

Actin networks rely on the actin binding proteins that contribute to the formation, arrangement, and function of the network. One such actin binding protein is the Arp2/3 complex,

which nucleates branched or dendritic actin networks by nucleating a daughter filament off the side of an existing mother filament. The dendritic networks nucleated by the Arp2/3 complex are primarily found to be responsible for functions that involve membrane remodeling, for example lamellipodia and endocytosis (Campellone and Welch 2010). The Arp2/3 complex from most eukaryotes consists of seven subunits: Arp2, Arp3, and ARPC1-5 (**Supplemental Figure 1**) and each subunit plays a specific role of varying importance in the nucleation process. ARPC2 and ARPC4 form the core of the complex and the primary contacts with the mother filament, Arp2 and Arp3 serve as the first subunits of the daughter filament, and ARPC1 and ARPC3 play a role in nucleation but are not critical for branch formation (Robinson et al. 2001; Gournier et al. 2001). Each of these subunits are found in *Chlamydomonas* but have varying degrees of sequence homology compared with conventional Arp2/3 complexes (**Supplemental Figure 1**). Interestingly, the ARPC5 subunit has yet to be found in *Chlamydomonas*. ARPC5 is thought to be important for the association of ARPC1 to the complex, but a mammalian complex lacking ARPC5 and ARPC1 maintains some nucleating and branching activity and is able to cross-link actin normally (Gournier et al. 2001).

Here, using the chemical inhibitor CK-666 to inhibit the nucleating function of the Arp2/3 complex (Hetrick et al. 2013) and a genetic mutant of a critical Arp2/3 complex member, ARPC4 (Cheng et al. 2017; Li et al. 2019), we take a more delicate approach to investigating the role of actin in ciliary assembly by separating different actin networks into their subfunctions based on topology. Specifically, we probe the involvement of actin networks nucleated by the Arp2/3 complex in ciliary maintenance and assembly. This approach in these cells has allowed us to propose a new model implicating a subset of filamentous actin in redistribution of membrane and proteins for the initial stages of ciliogenesis.

RESULTS

Loss of Arp2/3 complex function inhibits normal regeneration and maintenance of cilia:

To answer questions involving the role of Arp2/3 complex-mediated actin networks in ciliary assembly, we primarily used two tools. First, we used the chemical inhibitor CK-666 which blocks the nucleating ability of the Arp2/3 complex. Second, we obtained a null mutant of the critical Arp2/3 complex member, ARPC4 (Cheng et al. 2017; Li et al. 2019) from the *Chlamydomonas* Resource Center. This *arpc4* mutant was confirmed via PCR (**Supplemental Figure 2A**). We further evaluated this mutant by creating a genetic rescue where a V5-tagged ARPC4 construct is expressed in *arpc4* mutant cells, *arpc4:*ARPC4-V5. This was confirmed via PCR, western blot, and immunofluorescence (**Supplemental Figure 2**).

We first investigated the requirement for the Arp2/3 complex in maintenance of cilia by treating cells with varying concentrations of CK-666 or the inactive control CK-689 (250μM) for 2 hours and measuring the effect on steady state ciliary length. Consistent with previous results (Avasthi et al. 2014), we found that treating cells with CK-666 decreased ciliary length, suggesting that the Arp2/3 complex is required for maintaining cilia (**Figure 1A**). We saw no changes in ciliary length with the inactive CK-689 (**Figure 1A**) or when *arpc4* mutant cells lacking a functional Arp2/3 complex were treated with CK-666 (**Supplemental Figure 3**). Untreated *arpc4* mutant cells did however recapitulate the CK-666 result by showing a decreased ciliary length when compared with wild-type cells (**Figure 1B**). This defect in ciliary length was not present in the rescue, *arpc4:*ARPC4-V5 (**Figure 1B**). Overall, these results demonstrate through both chemical and genetic perturbation that the Arp2/3 complex is required for normal ciliary length maintenance.

Next, we probed the involvement of Arp2/3 complex-nucleated actin in the more complicated process of ciliary assembly where there is a high demand for protein and membrane both from pools already existing in the cell and from synthesis (Wingfield et al. 2017;

Nachury, Seeley, and Jin 2010; Rohatgi and Snell 2010; Jack et al. 2019; Diener, Lupetti, and Rosenbaum 2015). Cells were deciliated by low pH shock and then allowed to synchronously regenerate cilia after being returned to normal pH (Paul A. Lefebvre 1995). We found that cells lacking a functional Arp2/3 complex were slow to regenerate their cilia, and two-thirds of cells did not regrow cilia at all (**Figure 1C**). This phenotype could be rescued by expression of ARPC4-V5 in the *arpc4* mutant (**Figure 1D**). Importantly, the most severe defect in assembly appeared to be in the initial steps when existing protein and membrane are being incorporated into cilia.

The striking decrease in ciliary assembly is puzzling because the loss of Arp2/3 complex function, and therefore only a subset of actin filaments, results in a more dramatic phenotype than that of the *nap1* mutants treated with LatB, which are lacking all filamentous actins (Jack et al. 2019). However, in the *arpc4* mutant cells, a functional Arp2/3 complex never exists, and therefore, cells never have Arp2/3 complex-mediated actin networks. In *nap1* mutant cells treated with LatB, the treatment begins shortly after deciliation resulting in an acute perturbation. Further, LatB functions by sequestering actin monomers to promote filament disassembly, and thus the effects may not be immediate (Spector et al. 1989). Therefore, it is likely that there is a brief window where actin filaments can assert their initial role in ciliary regeneration before being depolymerized. To avoid this, we began the LatB treatment in *nap1* mutants 30 minutes before deciliation. This pre-treatment allows us to observe what happens when actin is not present immediately after deciliation. (**Figure 1E-F**). In this case, we see decreased ciliary length and dramatically decreased percent ciliation, which is consistent with the *arpc4* mutant results.

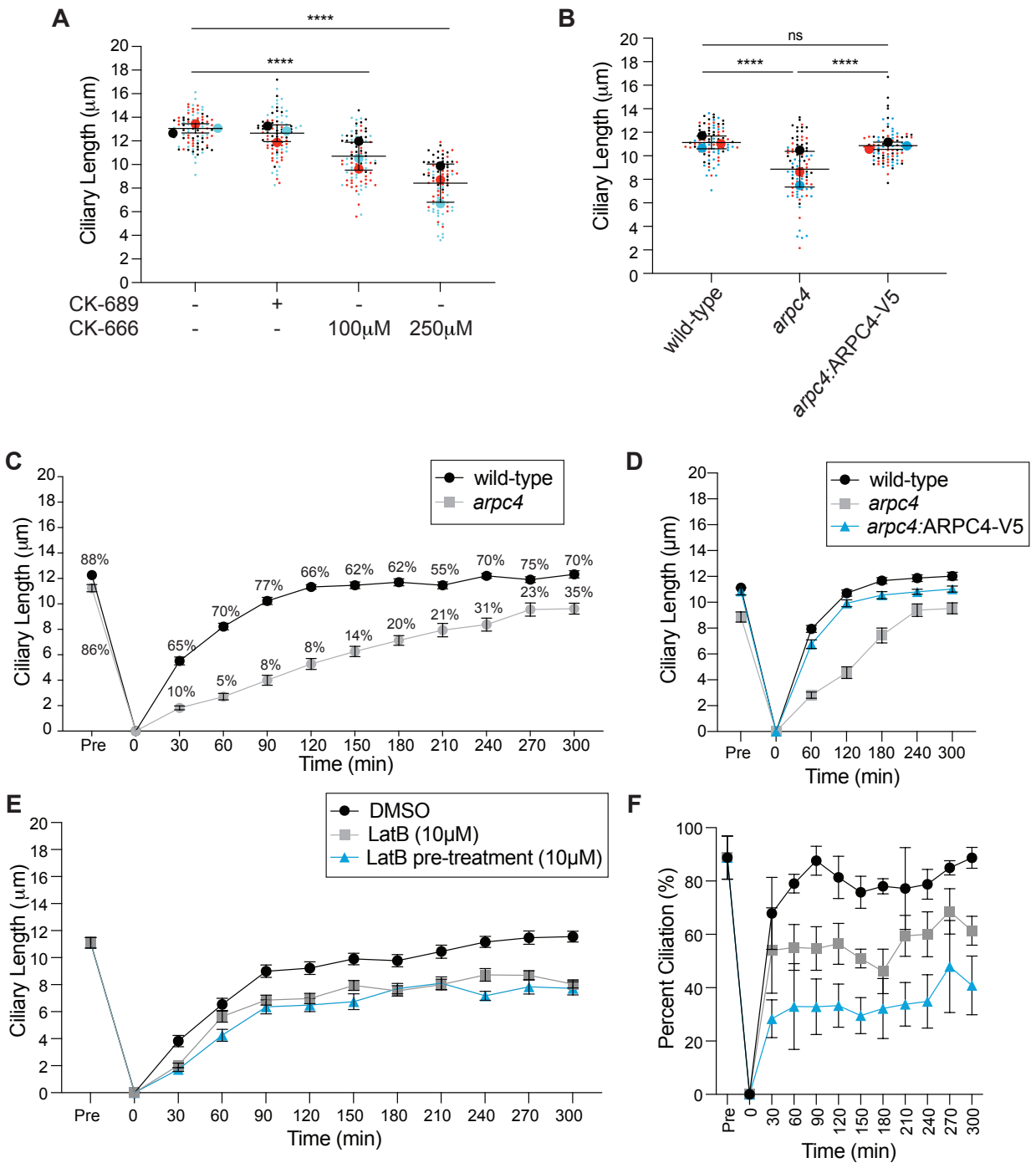

Figure 1. The Arp2/3 complex is required for normal ciliary maintenance and assembly. A) Wild-type cells were treated with 100μM or 250μM CK-666 or the inactive CK-689 for 2 hours. Cells were then imaged using a DIC microscope and cilia were measure in ImageJ. Superplots are used to show the mean of 3 separate experiments with error bars representing standard deviation. n=30 for each treatment in 3 separate experiments. P<0.0001. **B)** Wild-type cells, *arpc4* mutant cells, and *arpc4* mutant cells expressing *ARPC4-V5* steady state cilia were also measured with no treatment. Superplots are used to show the mean of 3 separate experiments with error bars representing standard deviation. n=30 for each strain for 3 separate experiments. P<0.0001. **C)** Wild-type cells and *arpc4* mutant cells were deciliated using a pH shock and then allowed to regrow. The black line represents wild-type, while the grey line represents the *arpc4* mutant. The numbers above or below each point show the percent ciliation for the wild-type and *arpc4* mutant cells respectively. Means are displayed with error bars representing 95% confidence interval. n=30 for

each strain and each time point in 3 separate experiments. For every time point except 0 min, P<0.0001 in terms of both length and percent ciliation. **D)** Wild-type cells, *arpc4* mutant cells, and *arpc4* mutant cells expressing *ARPC4-V5* were deciliated using a pH shock and then allowed to regrow. The black line represents wild-type, while the grey line represents the *arpc4* mutant and the cyan line represent the *arpc4* mutant expressing *ARPC4-V5*. Means are displayed with error bars representing 95% confidence interval. n=30 for each strain and each time point in 3 separate experiments. **E)** *nap1* mutant cells were pre-treated with 10μM LatB for 30 minutes before deciliation or treated with LatB upon the return to neutral pH following deciliation. The black line represents untreated cells, while the light grey line represents cells treated with LatB following deciliation and the dark grey line represents cells pre-treated with LatB. Error bars represent standard deviation. N=3 separate experiments. For every time point P>0.0001 between DMSO and treated samples, except 30min (10μM LatB) which is ns. **F)** Percent ciliation for the experiment in D. Line color is the same as D. Error bars represent standard deviation.

The Arp2/3 complex is required for the incorporation of existing membrane and proteins for ciliary assembly:

There are several distinct steps of ciliary assembly after severing, all of which require actin filaments. The first step requires that a pool of existing proteins and membrane are incorporated into cilia in an actin-dependent manner (Jack et al. 2019). As disruption of Arp2/3 complex-mediated actin networks results in slow initial ciliary assembly, when it is likely that existing protein is being incorporated, we questioned the involvement of Arp2/3 complex-dependent actin networks in the incorporation of existing ciliary protein.

By treating cells with cycloheximide (CHX), a protein synthesis inhibitor, we can eliminate the contribution of two steps in the process of ciliary assembly (**Figure 2A**) (Rosenbaum, Moulder, and Ringo 1969). Without protein synthesis, there is no trafficking or incorporation of new proteins. Therefore, any ciliary growth we see is due to the incorporation of the existing protein alone. Under normal conditions, cells that are deciliated and treated with cycloheximide typically grow cilia to about half-length, or 6μm, within 2 hours (**Figure 2B**). We also saw cells growing to half-length after 2 hours when treated with the inactive CK-689 and cycloheximide (**Figure 2B**). However, when treated with either 100μM or 250μM CK-666 and cycloheximide, cells exhibit a dose-dependent decrease in ciliary length after 2 hours of regeneration (**Figure 2B**).

To confirm the results of chemical perturbation, we used the *arpc4* mutant strain to genetically test the role of the Arp2/3 complex in incorporation of existing protein. When *arpc4* mutant cells were deciliated and treated with cycloheximide, they display minimal growth (**Figure 2C**). In fact, throughout a five-hour period, only 6% of cells were able to form cilia at all (**Figure 2C**). This suggests that the Arp2/3 complex and the actin networks nucleated by the complex are indispensable for the incorporation of existing protein and membrane during ciliary assembly. This can be further dissected because we know in the case of cells treated with cycloheximide and CK-666, the protein pool is available but is still not incorporated, suggesting a problem with membrane incorporation or delivery as opposed to a problem with protein availability.

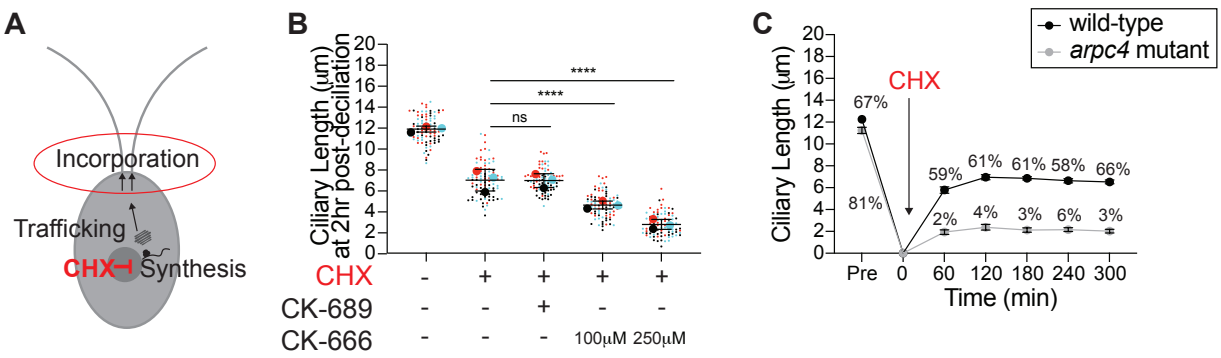

Figure 2. The Arp2/3 complex is required for incorporation of existing protein during ciliary assembly. A) Treating cells with cycloheximide inhibits protein synthesis, which means only incorporation of existing protein into the cilia is observed**. B)** Wild-type cells were deciliated and then treated with a combination of 10μM cycloheximide (CHX) and CK-666 (100μM or 250μM) or CK-689 (the inactive control) at the same concentration during regrowth. The graph shows the length of their cilia after 2 hours of treatment and regrowth. Superplots are used to show the mean of 3 separate experiments with error bars representing standard deviation. n=30 for each treatment group 3 separate experiments. For both the 100μM and 250μM CK-666 treatments with CHX, P<0.0001. **C)** Wild-type cells and *arpc4* mutants were deciliated and then allowed to regrow in 10μM CHX. The percentages above the lines represent the percent of cells with cilia at the indicated time points. The mean is shown with error bars representing 95% confidence interval. n=30 for each strain and each time point in 3 separate experiments. For every time point besides 0 min, P<0.0001 for both length and percent ciliation.

Cilia of *arpc4* mutant cells resorb faster in the absence of the Golgi:

Because we see defects in ciliary assembly and maintenance when cells are likely incorporating existing protein, and we know the protein needed for assembly is in excess due to our acute perturbations with CK-666, we next investigated membrane delivery to cilia. This is of particular interest as the Arp2/3 complex is canonically thought to be involved in membrane remodeling functions. Typically, the Golgi is known to be the main source of membrane for cilia (Nachury, Seeley, and Jin 2010; Rohatgi and Snell 2010), and both ciliary membrane, membrane proteins, and even axonemal proteins are transported in or attached to vesicles (Wood and Rosenbaum 2014). In *Chlamydomonas*, this has been demonstrated by the ciliary shortening of cells treated with Brefeldin A (BFA), a drug that causes Golgi collapse by interfering with ER to Golgi transport (W. Dentler 2013). To determine if the Arp2/3 complex is involved in the trafficking of new protein from the Golgi to cilia, we examined the Golgi following deciliation using transmission electron microscopy (TEM) in *arpc4* mutants (**Supplemental Figure 4A**). The Golgi appeared grossly normal, and in all cases had approximately the same number of cisternae (**Supplemental Figure 4A-B**) and did not show an abnormal accumulation of post-Golgi membrane as previously reported when perturbing all filamentous actin (Jack et al., 2019).

Alternative pathways for ciliary material have also been found in *Chlamydomonas*. For example, surface proteins were biotinylated and then cells were deciliated, meaning the membrane and proteins within cilia were lost. When cilia were allowed to regrow, biotinylated proteins were found to reside within the new cilia suggesting they came from the plasma membrane (W. Dentler 2013). Therefore, we hypothesized that due to its role in membrane remodeling, and particularly endocytosis, in other organisms, the Arp2/3 complex may be part of an endocytic pathway that provides membrane and perhaps membrane proteins to cilia (**Figure 3A**). To test if membrane could be coming from an endosomal or endocytic source other than the Golgi, we treated cells with 36μM BFA to collapse the Golgi and block exocytosis so cells would be forced to utilize other sources of ciliary proteins and membranes. Wild-type cells treated with BFA resorb slowly, but *arpc4* mutant cells had a faster resorption rate (**Figure 3B and D**). Further, the number of cells with cilia in the *arpc4* mutant cells dramatically decreased with BFA treatment (**Figure 3C**). Meanwhile, cells treated with other known ciliary resorption-inducing drugs that do not specifically target Golgi traffic, 3-isobutyl-1-methylxanthine (IBMX) (Pasquale and Goodenough 1987) or sodium pyrophosphate (NaPPi) (P. A. Lefebvre et al. 1978) show an increased velocity of resorption in the wild-type cells compared to the *arpc4* mutant cells (**Supplemental Figure 5**), suggesting the faster resorption of the *arpc4* mutant cells in BFA is specific to the effects of BFA on the cell. Thus, wild-type cells are more capable of maintaining cilia without membrane supply from the Golgi, suggesting that there must be another source for membrane that is dependent upon the Arp2/3 complex.

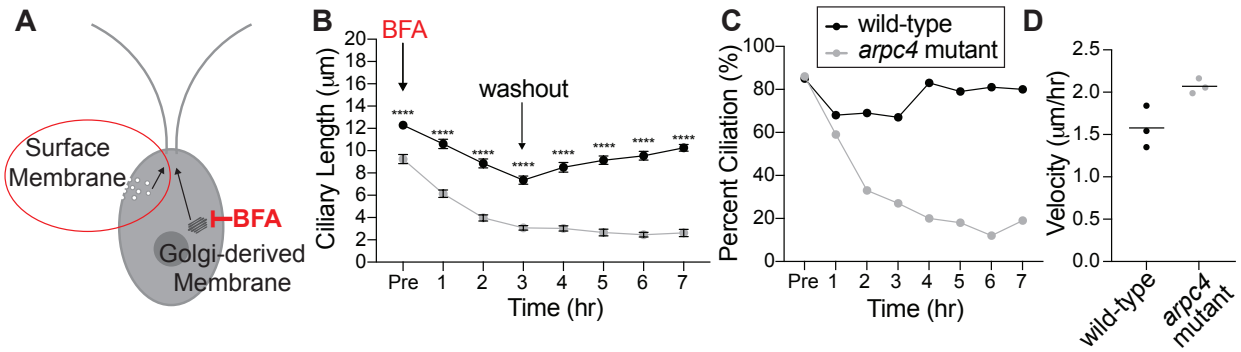

Figure 3. The Arp2/3 complex is required for ciliary maintenance in the absence of intact Golgi. A) Treating cells with Brefeldin A (BFA) causes the Golgi to collapse meaning any membranes and proteins used to maintain the cilia must come from other sources. **B)** Cells were treated with 36μM BFA for 3 hours at which time the drug was washed out. Wild-type is represented by black, while *arpc4* mutants are grey. The mean is shown with error bars representing 95% confidence interval. Error bars represent 95% confidence interval of the mean. n=30 for each time point and each strain in 3 separate experiments. **** represents P<0.0001. **C)** Percent ciliation of the cells in B. n=100. **D)** Resorption speed for wild-type cells and *arpc4* mutant cells as determined by fitting a line to the first 4 time points before washout and determining the slope of the line. Line represents the mean of 3 separate experiments. N=3. P=0.0314

Apical actin dots are dependent on the Arp2/3 complex:

Since ciliary membrane proteins can come from the Golgi or the plasma membrane and *arpc4* mutant cells have a more severe defect in incorporating ciliary proteins from non-Golgi sources, we asked if Arp2/3 complex-mediated actin networks might be responsible for endocytosis from the plasma membrane in *Chlamydomonas* as it is in other organisms. To determine where in the cell Arp2/3 complex-mediated actin networks might be acting, we looked directly at the effects of loss of Arp2/3 complex function on the actin structures in the cell. Using new protocols for the visualization of actin in *Chlamydomonas* developed by our lab (Craig et al. 2019), we stained wild-type cells and *arpc4* mutant cells with fluorescent phalloidin. In wild-type cells, apical dots reminiscent of endocytic actin patches in yeast are typically seen near the base of cilia (**Figure 4A**). We quantified the presence of these dots in the wild-type cells compared to the *arpc4* mutant cells (**Figure 4A-B**). We found that while about 70% of wild-type cells contain the dots, only about 5% of the *arpc4* mutant cells had dots (**Figure 4B**), suggesting the Arp2/3 complex is required for the formation of this actin structure. This phenotype was rescued by the expression of the ARPC4-V5 construct in the *arpc4* mutant cells (**Figure 4C**). The reliance of this structure on the Arp2/3 complex, led us to further question whether these dots could represent endocytic membrane remodeling.

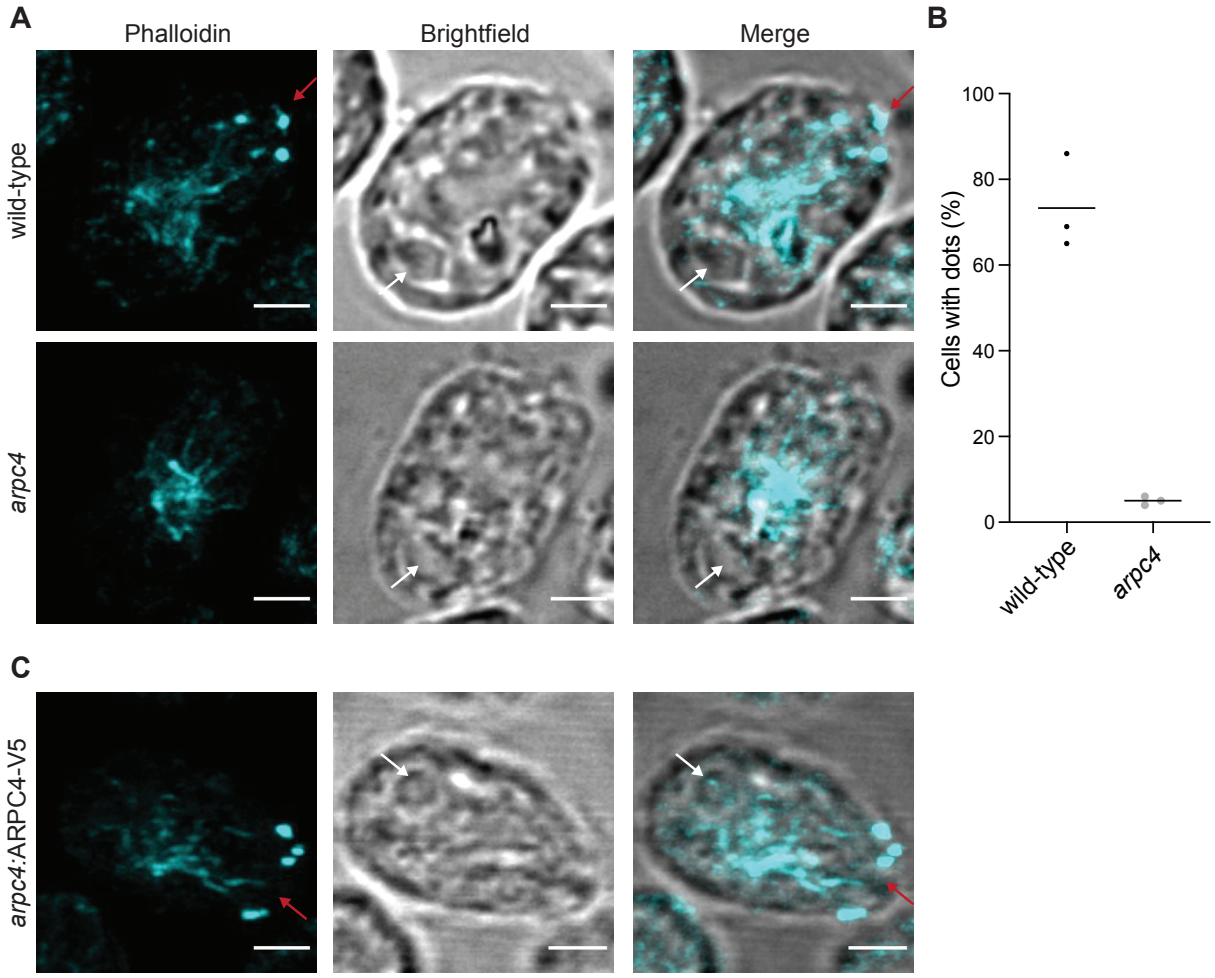

Figure 4. Loss of a functional Arp2/3 complex results in changes in actin distribution. A) Wild-type and *arpc4* mutant cells stained with phalloidin to visualize the actin network along with brightfield to show cell orientation. Images were taken as a z-stack using airsycan imaging and are shown as a maximum intensity projection. Red arrow is pointing to dots at the apex of the cell, and white arrow is pointing to the pyrenoid near the basal end of the cell. Scale bars represent 2μm. **B)** Percentage of cells with apical dots as shown in A. Percentages taken from 3 separate experiments where n=100. Line represents the mean. P<0.0001. **C)** Presence of apical dots in the *arpc4* mutant rescue expressing *ARPC4-V5*. Images were taken as a z-stack using airsycan imaging and are shown as a maximum intensity projection. Red arrow is pointing to dots at the apex of the cell, and white arrow is pointing to the pyrenoid near the basal end of the cell. Scale bars represent 2μm.

Endocytosis in *Chlamydomonas* is clathrin-dependent:

The Arp2/3 complex is conventionally thought to be involved in endocytosis in cell-walled yeast to overcome turgor pressure (Aghamohammadzadeh and Ayscough 2009; Basu, Munteanu, and Chang 2014; Carlsson and Bayly 2014). *Chlamydomonas* cells also have a cell wall and since the apical actin dots resemble these endocytic pits (Goode, Eskin, and Wendland 2015; Adams and Pringle 1984; Ayscough et al. 1997), we hypothesized that Arp2/3 complex and actin-dependent endocytosis might be occurring in *Chlamydomonas* even though this process has not yet been directly demonstrated in this organism. We compared the endocytosis-related proteins found in mammals and plants to those in *Chlamydomonas* (**Figure 5A**). We found that *Chlamydomonas* was lacking much of the important machinery for almost all typical endocytosis processes, including caveolin for caveolin-mediated endocytosis, flotillin for

flotillin-dependent endocytosis, and endophilin for endophilin-dependent endocytosis (**Figure 5A**). However, most of the canonical clathrin-related endocytosis machinery could be found in *Chlamydomonas*, and thus, clathrin-mediated endocytosis is conserved to a higher extent than other endocytic mechanisms.

We further probed the likelihood of clathrin-mediated endocytosis occurring in *Chlamydomonas* by treating cells with PitStop2 which inhibits the interaction of adaptor proteins with clathrin, halting clathrin-mediated endocytosis. For this experiment, we used the fixable lipophilic dye FM 4-46FX. This dye is impermeable to the plasma membrane but is usually quickly endocytosed into cells showing bright foci where dye is enriched in endocytosed compartments. Thus, we incubated the dye for only 1 minute to allow enough time for internalization into endosomes but not enough for incorporation into various cellular membrane structures. The ability of PitStop2-treated cells to internalize membrane was measured by calculating the total cell fluorescence inside the cell after allowing dye to be internalized (**Figure 5B**). We found that cells treated with 30μM PitStop2 have significantly decreased membrane internalization, meaning clathrin is required for the internalization of this membrane dye (**Figure 5C**), which further supports the idea that clathrin-mediated endocytosis is occurring in *Chlamydomonas*.

Next, we tested whether the endocytosis is Arp2/3 complex-dependent by using this membrane internalization assay on *arpc4* mutant cells compared to wild-type cells. We found that cells lacking a functional Arp2/3 complex have decreased total cell fluorescence (**Figure 5D-E**) suggesting the clathrin-mediated endocytosis in *Chlamydomonas* is Arp2/3 complex-dependent.

To confirm that clathrin mediated endocytosis is being inhibited by both PitStop2 and the loss of the Arp2/3 complex

better demonstrate the relationship between the Arp2/3 complex and clathrin mediated endocytosis, we used a clathrin light chain antibody to stain cells. In both PitStop2 treated cells and *arpc4* mutant cells, but not in untreated wild-type cells, we see a mislocalization of clathrin staining around the pyrenoid (**Supplemental Figure 6, Figure 5F-G**). Although the reason for this accumulation of clathrin around the pyrenoid is not clear, the interesting takeaway from this data is that disruption of either clathrin mediated endocytosis with PitStop2 or of Arp2/3 function results in defects in membrane internalization and clathrin localization. These data support a role for the Arp2/3 complex in clathrin-mediated endocytosis.

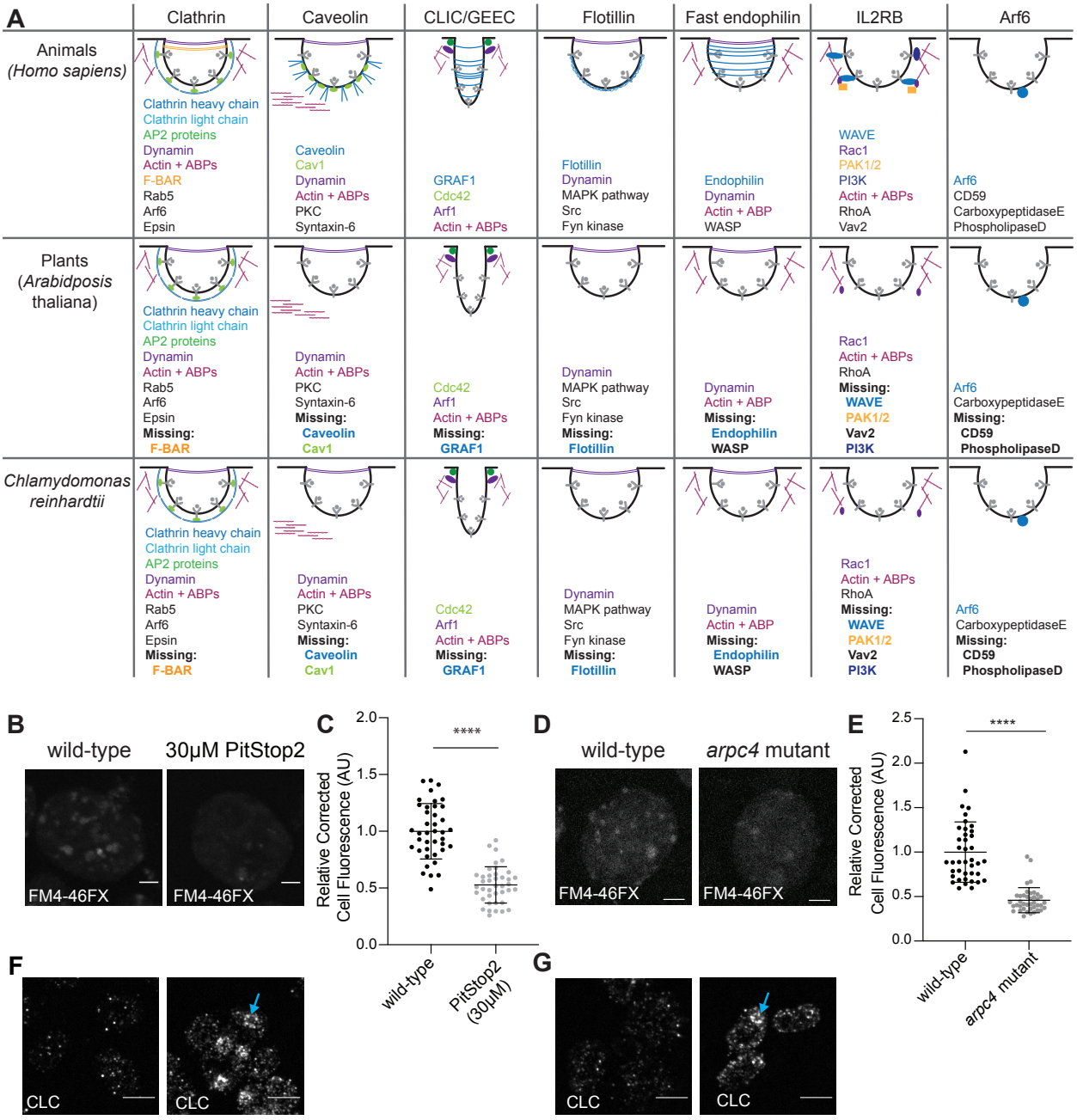

Figure 5. Arp2/3 complex-dependent clathrin-mediated endocytosis is conserved in *Chlamydomonas*. A) Gene presence was determined using BLAST. Word colors correspond to diagram colors. **B)** Cells treated with 30μM PitStop2 were incubated with FM4-46FX and imaged on a spinning disk confocal. Max intensity projections of z-stacks are shown. Scale bars are 2μm. **C)** The background corrected fluorescence for each sample. The mean is shown with error bars showing standard deviation. n=40 in 3 separate experiments. P<0.0001. **D)** Wild-type and *arpc4* mutant cells treated with FM4-46FX and imaged on a spinning disk confocal. Max intensity projections of z-stacks are shown. Scale bars are 2μm. **E)** The background corrected fluorescence for each sample. The mean is shown with error bars representing standard deviation. n=30 in 3 separate experiments. P<0.0001. **F)** Wild-type and PitStop2 treated cells, and arpc4 mutant cells were stained with clathrin light chain antibody and imaged using a spinning disk confocal. Cyan arrows point to accumulation around the pyrenoid. Scale bar represents 5μm. **G)** Wild-type and arpc4 mutant cells were stained with clathrin light chain antibody and imaged using a spinning disk confocal. Cyan arrows point to accumulation around the pyrenoid. Scale bar represents 5μm.

The Arp2/3 complex is required for the internalization and relocalization of a membrane protein from the periphery of the cell to cilia:

Upon finding that there is likely Arp2/3 complex-dependent clathrin-mediated endocytosis in *Chlamydomonas*, we next asked if this endocytosis could be responsible for the relocalization and internalization of a known ciliary protein. SAG1 is a membrane protein that is important for mating in *Chlamydomonas* cells (Belzile et al. 2013). When cells are induced for mating with dibutyryl-cAMP (db-cAMP), SAG1 must relocalize from the cell periphery to cilia, where it facilitates ciliary adhesion between mating cells. This relocalizaiton of SAG1 is thought to occur through internalization of the protein followed by internal trafficking on microtubules to the base of cilia (Belzile et al. 2013).

We examined whether actin and the Arp2/3 complex were required for the transport of HA-tagged SAG1 to the apex of the cell and cilia for agglutination during mating (**Figure 6A**). Using immunofluorescence, we observed cells treated with either 10μM LatB to depolymerize IDA5 or 250μM CK-666 to perturb the Arp2/3 complex. Before induction, SAG1-HA localized to the periphery of the cell (**Figure 6B, top**). 30 minutes after induction with db-cAMP, SAG1-HA relocalized to the apex of the cell and to cilia in untreated cells (**Figure 6B, left**). In both LatB and CK-666 treated cells, this apical enrichment was greatly decreased (**Figure 6B, middle and right**). To quantify this, line scans were drawn through the cell from the apex to the basal region (**Figure 6C-D**). The percentage of cells with apical enrichment was calculated, and it was found that untreated cells had a higher percent of apical enrichment when compared with LatB or CK-666 treated cells (**Figure 6E**). Thus, cells with perturbed Arp2/3 complex-mediated filamentous actin show decreased efficiency of SAG1-HA relocalization.

We next asked if this decrease in relocalization in cells with actin and Arp2/3 complex inhibition could be due to a decrease in the internalization of SAG1-HA through a process that seems to require endocytosis. To investigate this, we used a method first described by Belzile et al. 2013, where cells were induced and treated with a low percentage (0.01%) of trypsin, which will hydrolyze exterior proteins but cannot enter the cell. In untreated cells, we see an increase in SAG1-HA protein levels following induction because SAG1-HA is internalized and becomes protected from trypsin (**Figure 6F**). In cells treated with either 10μM LatB or 250μM CK-666 we see a decrease in this trypsin protection as shown in the western blot (**Figure 6F**). This was further quantified by subtracting the amount of protein before induction from the amount of protein present after induction, which gives a value representing the amount of SAG1-HA protected from trypsin due to internalization in these cells (**Figure 6G**). The decrease in SAG1-HA following induction in cells with decreased filamentous actin and Arp2/3 complex function indicates a role for Arp2/3 complex-mediated actin networks in internalization of this specific ciliary membrane protein.

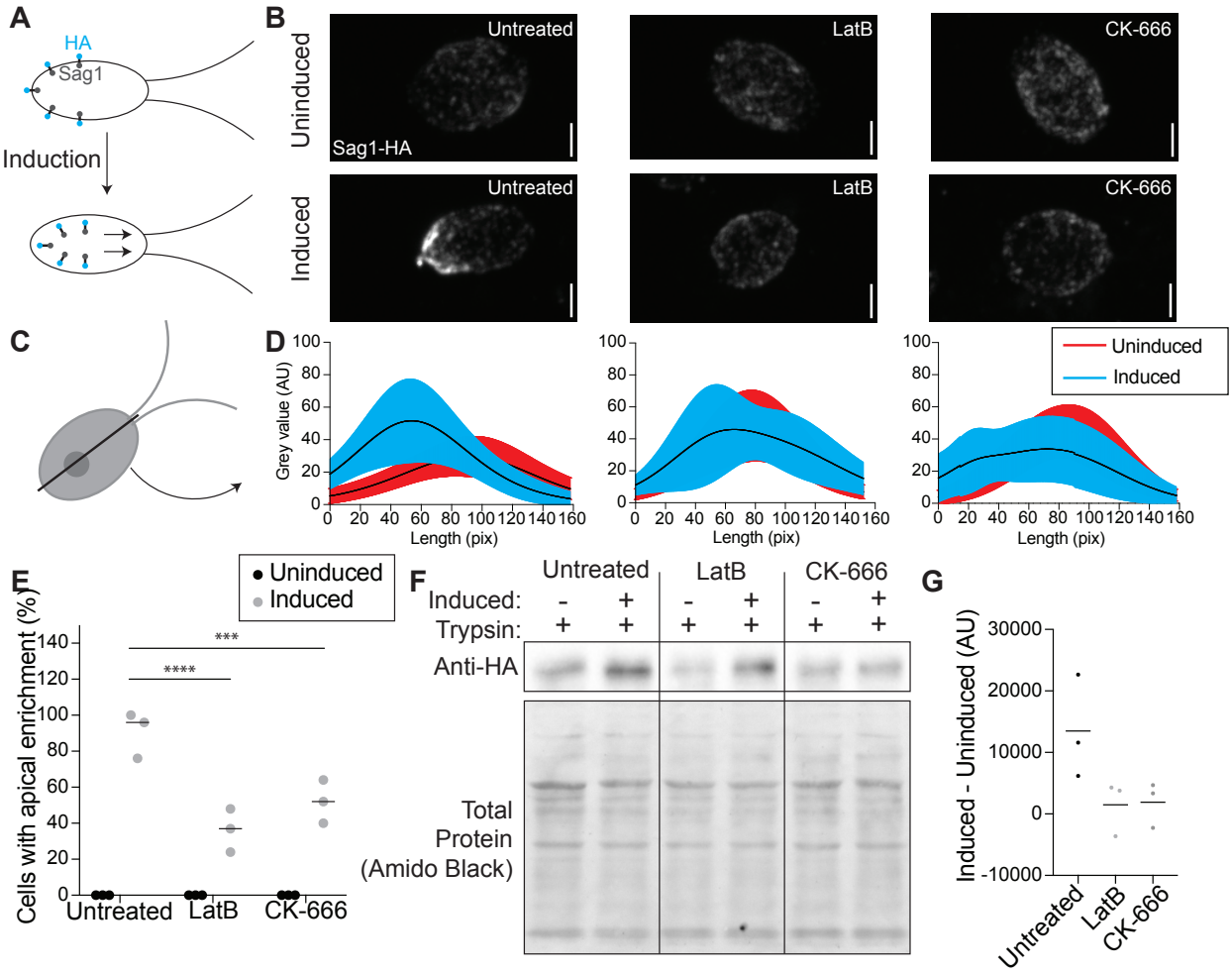

Figure 6. The Arp2/3 complex is required for the relocalization and internalization of the ciliary protein SAG1 for mating. A) When mating is induced SAG1-HA is internalized and relocalized to the apex of the cells and cilia for agglutination. **B)** Maximum intensity projections of z-stacks taken using spinning disk confocal microscopy of SAG1-HA. Left is untreated, middle is treated with 10μM LatB, and right is treated with 250μM CK-666. Top row of images are uninduced and bottom row of images are induced with db-cAMP. Scale bar represents 2μm. **C)** Diagram representing line scans taken through the cells in z-stack sum images. **D)** Line scans were taken from the apex of the cell to the basal region of the cell in untreated cells (left), LatB treated cells (middle), and CK-666 (right). Lines scans were normalized and fit with a gaussian curve. The curves were averaged. Black lines represent mean and then shaded regions represent standard deviation. Grey represents uninduced samples, green represent induced samples. 0 on the y-axis represents the apical region of the cell. n=30 from a single representative experiment. **E)** Percentage of cells with apical enrichment based on E for uninduced (black) and induced (grey) cells for each treatment group. The mean is shown with error bars representing standard deviation. n=30 for 3 separate experiments for each treatment. **F)** Western blot showing amount of SAG1-HA in uninduced and induced cells in each treatment group all treated with 0.01% trypsin. **G)** Intensity of the bands in H were normalized to the total protein as determined by amido black staining and quantified in ImageJ was used to subtract uninduced from induced to give a representation of the amount of SAG1-HA internalized with induction. Line represents mean of 3 separate experiments.

Actin dots increase in an Arp2/3 complex and clathrin-dependent manner following deciliation:

Having established that the Arp2/3 complex is required for ciliary assembly, membrane dye internalization, and the endocytosis of a known ciliary protein, we wondered if these functions could be connected given that *arpc4* mutant cells have defects in maintaining cilia

from non-Golgi sources (**Figure 3**). Therefore, we returned to the Arp2/3 complex-dependent actin dots seen in wild-type cells that are reminiscent of endocytic pits in yeast. Because ciliary membrane and proteins can come from the plasma membrane (Dentler, 2013), we suspected there would be an increase in these actin dots immediately following deciliation. We used phalloidin to visualize the actin cytoskeleton of wild-type cells before and immediately following deciliation, as well as 10 minutes later (**Figure 7A**). We saw an increase in both the percentage of cells with dots and the number of dots per cell immediately following deciliation that then returned to normal by 10 minutes (**Figure 7A and D**). This is consistent with the results shown in **Figure 1E-F** and confirms that the defect seen in ciliary assembly is due to an event occurring very early in ciliary assembly, even within the first few minutes after deciliation.

We wondered if this increase in dots would result in dots in the *arpc4* mutant cells which have almost not dots normally. We found that in the *arpc4* mutants dots were never observed, before or after deciliation (**Figure 7B and D**), suggesting these dots are dependent on the Arp2/3 complex. Next, we wanted to see if the dots really were due to clathrin-mediated endocytosis, so we treated cells with PitStop2 and looked for this same increase in dots. This treatment almost fully blocked the appearance of dots following deciliation and completely eliminated the presence of cells with 3 or more dots (**Figure 7C-D**), suggesting a clathrin-dependent mechanism, as well as an Arp2/3-dependent mechanism, is related to these dots.

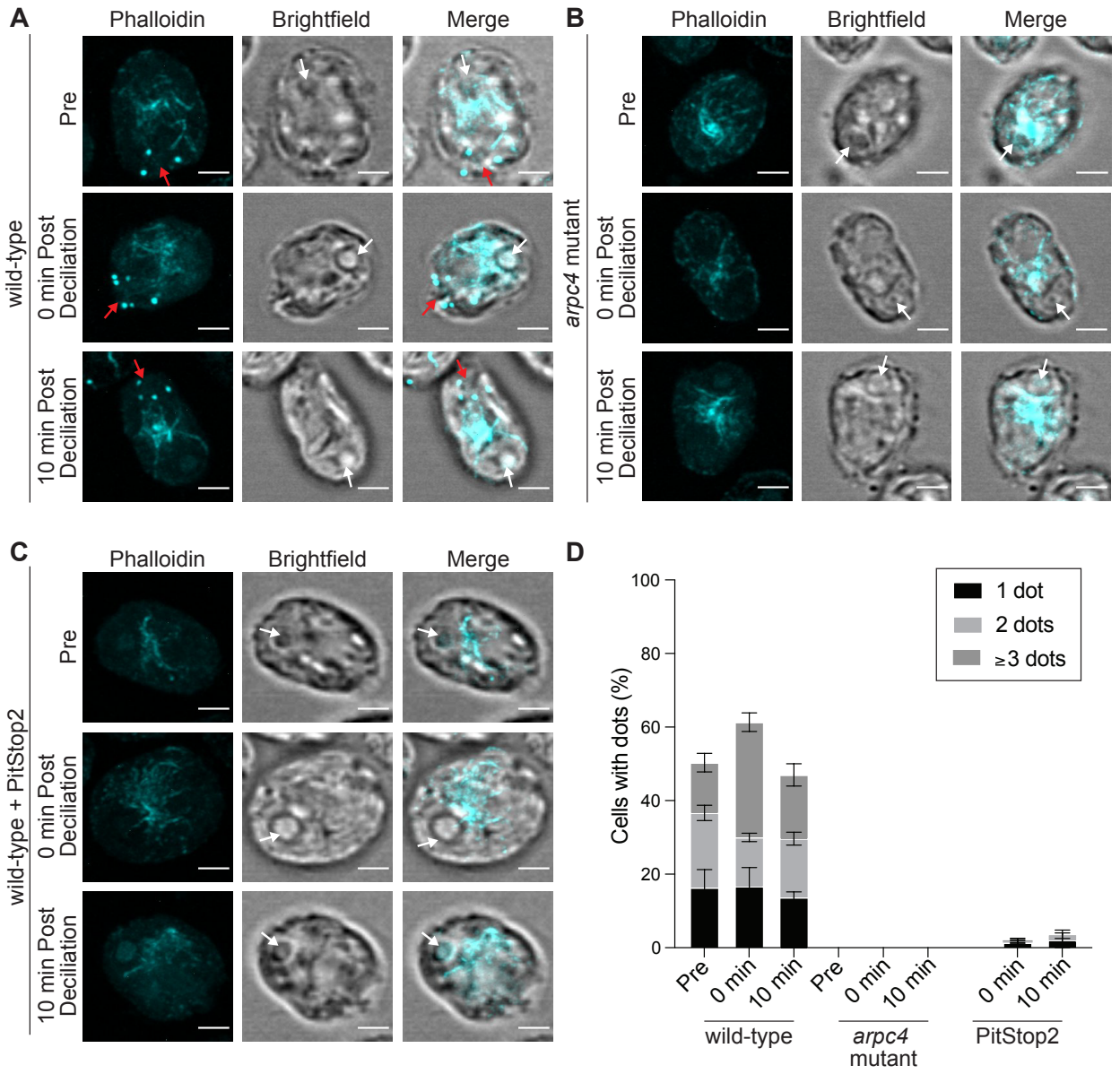

Figure 7. Actin dots are clathrin and Arp2/3 complex-dependent. A-C) Wild-type cells **(A)**, *arpc4* mutant cells **(B)**, and wild-type cells treated with 30 μM PitStop2 **(C)** stained with phalloidin to visualize the actin network before deciliation, immediately following deciliation, and 10 minutes following deciliation. Brightfield images are to visualize cell orientation. Images were taken as a z-stack using airyscan imaging and are shown as a maximum intensity projection. Scale bar represents 2μm. Red arrows point to dots at the apex of the cell, and white arrows point to the pyrenoid at the opposite end of the cell. **D)** The percentage of cells with 1 dot, 2 dot, or 3 dots in each condition. Quantification based on sum slices of z-stacks taken using a spinning disk confocal. n=100 in 3 separate experiments.

Ciliary membrane proteins follow different paths from the plasma membrane to the cilia: Finally, to specifically determine if ciliary membrane and therefore membrane proteins were coming from a pool in the plasma membrane we did an experiment first described in W. Dentler 2013. Surface proteins were biotinylated, then cells were deciliated. After the cilia regrew, they were isolated and probed for biotinylated protein (**Figure 8A**). Any biotinylated protein present in the newly grown and isolated cilia must have come from a pool in the plasma membrane. While some proteins returned in both wild-type and *arpc4* mutant cells, some

appeared to a lesser degree in *arpc4* mutant cells compared to wild-type cells (**Figure 8B-E, black arrow and black bars**) and some returned to a higher degree in *arpc4* mutant cells (**Figure 8B-E, grey arrow and grey bars**). Other biotinylated proteins found in wild-type cilia were not found in the *arpc4* mutant cilia before or after deciliation, so there is a mechanism for delivery of proteins to the cilia from the plasma membrane that Arp2/3 is absolutely essential for (**Figure 8B-C**). This suggests there are multiple paths to the ciliary membrane, some of which are Arp2/3 complex-independent and some that are Arp2/3 complex-dependent. This may represent lateral diffusion and endocytosis respectively.

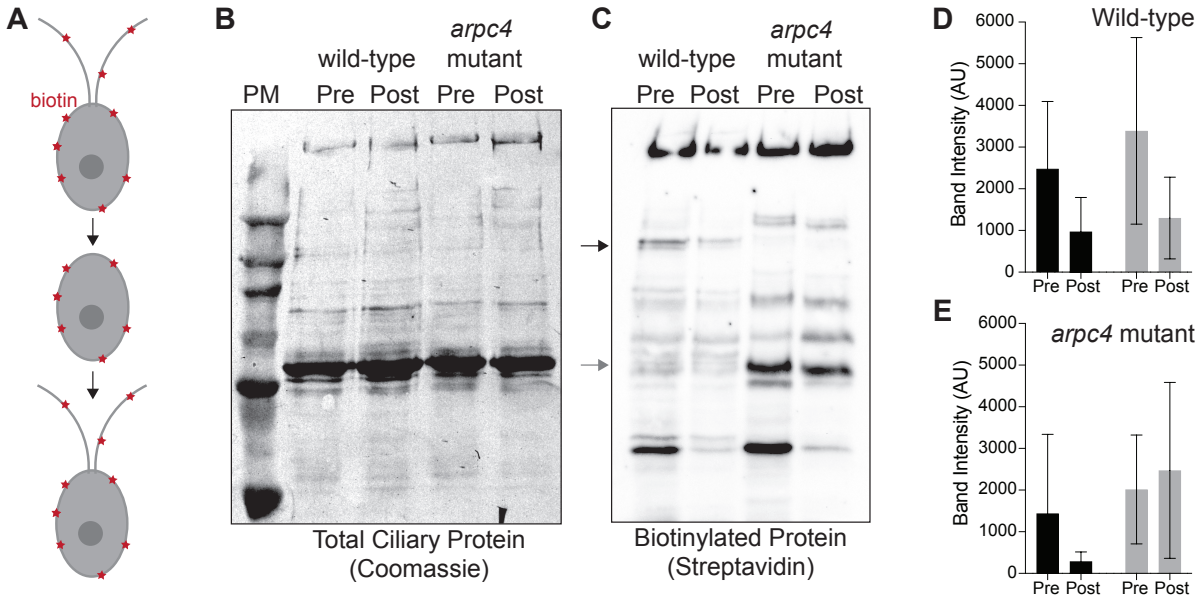

Figure 8. Ciliary membrane proteins have multiple paths from the plasma membrane. A) Cells were biotinylated, deciliated, and then allowed to regrow before cilia were isolated and probed for biotinylated protein**. B)** Total protein in wild-type and *arpc4* mutant ciliary isolate investigated by western blot and Coomassie. **C)** Wild-type and *arpc4* mutant cells ciliary isolate was investigated by western blot and probed using streptavidin. Black arrow shows ciliary protein present to a higher degree in wild-type cells than the *arpc4* mutant cells. Grey arrows show ciliary protein that is present to a higher degree in *arpc4* mutant cells than in wild-type cells. **D)** Bands represented by black and grey arrows are quantified for the wild-type cells. Data acquired from 3 separate experiments. **E)** Bands represented by black and grey arrows are quantified for the *arpc4* mutant cells. Data represented as the mean from 3 separate experiments. Error bars represent standard deviation.

DISCUSSION

In this study, we investigate the Arp2/3 complex of *Chlamydomonas reinhardtii* that functions to maintain and assemble cilia. This complex potentially lacks the ARPC5 subunit, although it is possible that a highly divergent ARPC5 exists. In yeast, deletion of any of the genes encoding Arp2/3 complex members causes severe defects and even lethality, but these defects differ in severity depending on the complex members deleted, suggesting that complex members have varying degrees of importance in Arp2/3 complex function (Winter, Choe, and Li 1999). The role of ARPC5 in actin nucleation is being investigated, but some groups have found it unnecessary for overall function of the complex (Gournier et al. 2001; von Loeffelholz et al. 2020). Furthermore, our data show that knocking out function of the ARPC5-less *Chlamydomonas* Arp2/3 complex genetically or chemically results in phenotypes in ciliary assembly and maintenance, suggesting that the wild-type complex is active. Because the Arp2/3 complex has known functions in membrane dynamics, this led us to pursue models of Arp2/3 complex-dependent membrane trafficking to cilia.

Previously, three models for the trafficking of membrane proteins to cilia have been proposed (Nachury, Seeley, and Jin 2010). The first is that Golgi vesicles containing ciliary proteins are docked at the base of the cilium and fuse with the ciliary membrane inside the cilium itself. Proteins, both membrane and axonemal, have been found to be transferred from the Golgi to the cilia on or in cytoplasmic vesicles (Wood and Rosenbaum 2014). Second, Golgi vesicles containing ciliary proteins are docked near the base of the cilium still within the diffusion barrier (Papermaster, Schneider, and Besharse 1985; Nachury et al. 2007; Zuo, Guo, and Lipschutz 2009). In *Chlamydomonas*, this was first described for mastigoneme proteins, which were found to be transferred from the Golgi and then exocytosed for use on the exterior of the cell (Bouck 1971). In the third model, Golgi vesicles containing proteins fuse with the plasma membrane and membrane proteins are then somehow moved across this barrier within the plasma membrane, perhaps through lateral diffusion. Evidence for this path was shown using Hedgehog signaling protein Smoothened, which was found to relocalize in a dynamin-independent manner from the plasma membrane to the cilia immediately after stimulation in pulse labeling studies (Milenkovic, Scott, and Rohatgi 2009).

Our data support a fourth model, likely occurring in concert with other models, in which membrane proteins are recruited to the cilium from a reservoir in the cell body plasma membrane. We find that immediately following deciliation the Arp2/3 complex is required for ciliary assembly, clathrin-mediated endocytosis, and redistribution of ciliary proteins from the plasma membrane (**Figure 9A**). We hypothesize that ciliary membrane proteins and membrane targeted to the plasma membrane of the cell outside the diffusion barrier can be endocytosed and trafficked to cilia, either within or outside of the diffusion barrier in an actin and Arp2/3 complex-dependent manner.

Although our data does not eliminate the possibility of Arp2/3 complex function in supply of ciliary membrane and protein stored in other endosomal compartments, ciliary localization of proteins initially labeled on the cell surface with biotin (**Figure 8**) suggests that some ciliary membrane proteins incorporated during assembly are coming directly from the plasma membrane itself. An endocytic mechanism of trafficking in intracellular ciliogenesis has been investigated previously in mammalian RPE1 cells. The ciliary pocket found at the base of primary and motile cilia formed intracellularly has been found to be an endocytically active region (Molla-Herman et al. 2010) but clathrin-mediated endocytosis was not required for ciliogenesis in those cells. The Bardet Biedl Syndrome complex (BBsome), which is involved in regulation of ciliary membrane protein composition, has been shown to interact with clathrin directly at the ciliary pocket to facilitate membrane sorting in trypanosomes (Langousis et al. 2016). Further, some BBsome complex members resemble coat proteins such as clathrin (Jin et al. 2010) suggesting a direct role for the this cilium regulatory complex in membrane budding functions. Even in *Chlamydomonas*, clathrin heavy chain has been found to localize at the base of cilia (Kaplan et al. 2012). While the mechanism was unknown, it has been shown that plasma membrane surface-exposed proteins are relocalized to cilia during ciliary regeneration (W. Dentler 2013), a result we were able to recapitulate and demonstrate depends, in part, upon the Arp2/3 complex.

Altogether, this leads us to hypothesize that the role of the Arp2/3 complex in ciliary assembly is through endocytic recruitment from a ciliary protein reservoir in the plasma membrane before newly synthesized protein and Golgi-derived membrane are capable of supplying additional materials (**Figure 9B**). While this model provides a possible route that some ciliary proteins and membranes take to the cilia, we believe this is one of several paths that can be taken to the cilia. Trafficking to cilia is likely cargo- and time-dependent, and which path proteins take may tell us the order and speed in which they populate the cilium for subsequent function.

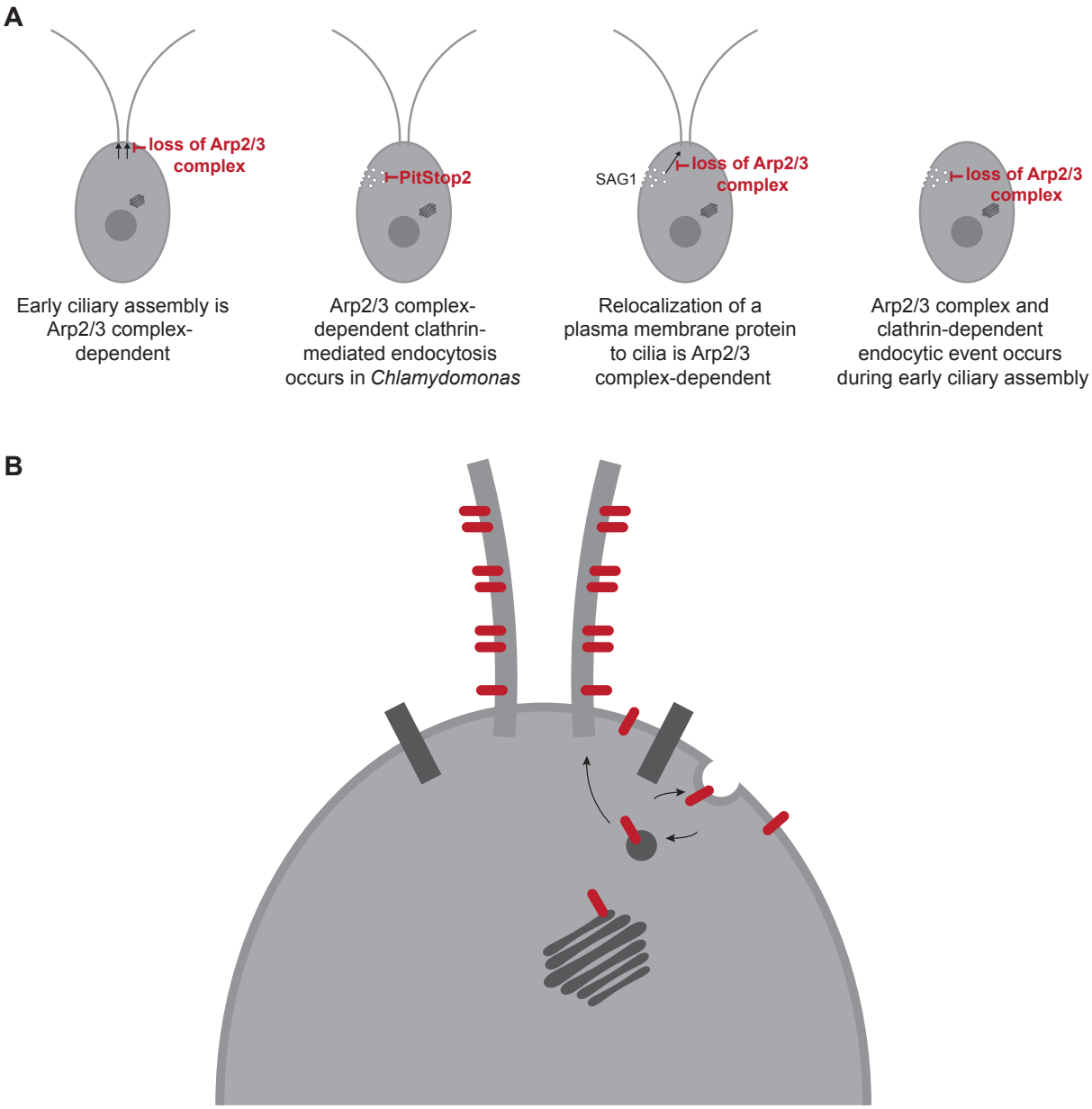

Figure 9. The Arp2/3 complex is required for membrane and protein delivery via a Golgi-independent, endocytosis-like process. A) Arp2/3-mediated actin networks are required for ciliary assembly in *Chlamydomonas* particularly during the initial stages. These actin networks are also required for clathrin-mediated endocytosis, and for the endocytosis-like relocalization of a ciliary protein from the plasma membrane to the cilia. Finally, a large endocytic event occurs immediately following deciliation that is Arp2/3 complex-mediated and dependent on clathrin-mediated endocytosis. **B)** Proposed model of membrane protein and membrane transport from the plasma membrane to the cilia through endocytosis.

METHODS

Strains:

The wild-type *Chlamydomonas* strain (CC-5325) and the *arpc4* mutant (LMJ.RY0402.232713) from the *Chlamydomonas* resource center. The *nap1* mutant was a gift from Fred Cross, Masayuki Onishi, and John Pringle. The SAG1-HA strain was a gift from William Snell. Cells were grown and maintained on 1.5% Tris-Acetate Phosphate Agar (TAP) plates (*Chlamydomonas* resource center) under constant blue (450-475 nm) and red light (625-660 nm). For experiments, cells were grown in liquid TAP media (*Chlamydomonas* resource center) overnight under constant red and blue light with agitation from a rotator. To induce gametes for mating for the SAG1-HA experiments, cells were grown in liquid M-N media (*Chlamydomonas* resource center) overnight with constant red and blue light and agitation.

Ciliary studies:

For steady state experiments, cells were treated with specified drugs [either 100μM CK-666, 250μM CK-666 (Sigma, Burlington, MA), 250μM CK-689 (Sigma, Burlington, MA), 10μM LatB (Sigma, Burlington, MA), 10μM CHX (Sigma, Burlington, MA), or 36μM BFA (Sigma, Burlington, MA)] and incubated with agitation for the allotted times. Following any incubation (as well as a pre sample), cells were diluted in an equal volume of 2% glutaraldehyde and incubated at 4º Celsius until they sediment. Following sedimentation, cells were imaged using a Zeiss DIC scope with a 40X objective. Cilia were then measured using the segmented line function in ImageJ.

For regeneration experiments, a pre sample was taken by adding cells to an equal volume of 2% glutaraldehyde. Then cells were deciliated with 115μL of 0.5N acetic acid for 45 seconds. After this short incubation, the pH was returned to normal by adding 120μL of 0.5N KOH. A 0-minute sample was again taken by adding cells to an equal volume of 2% glutaraldehyde. Then cells were incubated with agitation and allowed to regrow cilia for the allotted time period with samples taken at the indicated time points by adding cells to an equal volume of 2% glutaraldehyde. Cells in glutaraldehyde were allowed to incubate at 4º Celsius until sedimentation. Then, cells were imaged using the same Zeiss DIC scope with a 40X objective. Cilia were then measured using the segmented line function in ImageJ.

Phalloidin staining and quantification:

Procedure adapted from (Craig et al. 2019). Cells were mounted onto poly-lysine coverslips and fixed with fresh 4% paraformaldehyde in 1X HEPES. Coverslips with cells were then permeabilized with acetone and allowed to dry. Cells were rehydrated with PBS, stained with atto-phalloidin-488 (Sigma, Burlington, MA), and finally washed with PBS and allowed to dry before mounting with Fluoromount-G (Craig et al. 2019). Cells were imaged using the Nikon Spinning Disk Confocal. Z-stacks were obtained, and in ImageJ, maximum intensity projections were created for viewing.

Electron microscopy:

Cells (1mL of each strain) were deciliated via pH shock by adding 115μL of 0.5N acetic acid for 45 seconds followed by 120μL of 0.5N KOH to bring cells back to neutral pH. Cells were allowed to regrow cilia for 30 minutes. A pre sample and a 30-minute post-deciliation sample were fixed in an equal volume of 2% glutaraldehyde for 20 minutes at room temperature. Samples were then pelleted using gentle centrifugation for 10 minutes. The supernatant was removed, and cells were resuspended in 1% glutaraldehyde, 20mM sodium cacodylate. Cells were incubated for 1 hour at room temperature and then overnight at 4º Celsius. This protocol was first reported in (W. L. Dentler and Adams 1992).

SAG1-HA Immunofluorescence:

Procedure adapted from (Belzile et al. 2013). SAG1-HA cells were grown overnight in M-N media to induce gametes. These cells were then treated with either 10μM LatB for 1 hour or 250μM CK-666 for 2 hours. Following treatment, mating was induced by adding db-cAMP (ChemCruz, Santa Cruz, CA) to a final concentration of 13.5mM and incubating for 30 minutes. Cells were adhered to coverslips and fixed with methanol. Cells were then dried and rehydrated with PBS and incubated with 100% block (5% BSA, 1% fish gelatin) for 30 minutes. The 100% block was replaced with new 100% block containing 10% normal goat serum for another 30-minute incubation. The primary antibody (rat anti-HA, Sigma, Burlington, MA) was diluted 1:1000 in 20% block in PBS. Coverslips were incubated at 4º Celsius in a humidified chamber overnight. The primary antibody was removed and washed away with 3 10-minute PBS washes. The secondary (anti-rat IgG-Alexafluor 488, Invitrogen, Carlsbad, CA) was added and coverslips were incubated at room temperature for 1 hour. This was followed by 3 more 10-minute PBS washes and finally mounting with Fluoromount-G. Cells were imaged using a Nikon widefield microscope. Z-stacks were obtained, and maximum intensity projections were created for visualization and sum slices were created for quantification using ImageJ.

Images were quantified by using line scans from the apex of the cells to the basal region of the cells farthest away from the apex. Line scans were then normalized, and background subtracted before being combined into single graphs. Using the line scans, the intensity of signal at the basal region of the cells was subtracted from the signal at the apical region. Finally, cells with a difference over 30 were considered to be apically enriched and this was quantified as percentage of cells with apical staining.

SAG1-HA western blot:

Procedure adapted from (Belzile et al. 2013). SAG1-HA cells were grown overnight in M-N media to induce gametes. These cells were then treated with either 10μM LatB for 1 hour or 250μM CK-666 for 2 hours. Following treatment, mating induction was done by adding db-cAMP to a final concentration of 13.5mM and incubating for 10 minutes. Cells were then treated with 0.01% trypsin for 5 minutes, pelleted (at 500xg for 2 minutes), resuspended in lysis buffer (5% glycerol, 1% NP-40, 1mM DTT, 1X protease inhibitors), and then lysed with bead beating. Cell debris was spun down at 14000xg for 15 minutes. An equal amount of protein was loaded to a 10% SDS-PAGE gel. The resulting gel was transferred to membrane which was then blocked with 5% milk in PBST. The primary antibody (rabbit anti-HA, Cell Signaling, Danvers, MA) diluted to 1:1000 in 1% BSA, 1% milk was added and incubated overnight at 4º Celsius. Primary antibody washed off with 3 10-minute PBST washes. Secondary antibody (anti rabbit IgG, Invitrogen, Carlsbad, CA) was diluted to 1:5000 in 1% milk. 1% BSA was added, and the blot was incubated for 1 hour. Membrane was probed with West Pico Chemiluminescent Pico Substrate (Invitrogen, Carlsbad, CA). The same membrane was stripped of antibody and total protein was determined with amido black staining. Band intensity was measured in ImageJ and normalized to total protein

Membrane stain:

FM 4-64FX membrane stain (Thermo, Waltham, MA) was diluted to a stock concentration of 200μg/mL. Cells were adhered to poly-lysine coverslips. After a 5-minute incubation, cells were tilted off and 5μg/mL of ice-cold stain in Hank's Buffered Salt Solution (HBSS) without magnesium or calcium was added for 1 minute. The stain was tilted off and cells were fixed with ice cold 4% paraformaldehyde in HBSS without magnesium or calcium for 15 minutes. Coverslips were then rinsed 3 times for 10 minutes each in ice cold HBSS without magnesium

or calcium. Finally, cells were mounted with Fluoromount-G and imaged using the Nikon Spinning Disk Confocal. Z-stacks were taken and combined into sum projections using ImageJ. The background corrected total cell fluorescence was then calculated by taking the integrated density and subtracting the sum of the area and the mean background intensity.

Clathrin light chain immunofluorescence:
Cells were grown overnight in TAP media. Cells were deciliated using low pH shock. Cells are then adhered to coverslips and fixed with 4% PFA in 1X HEPES. Cells were then dried and rehydrated with PBS and incubated with 100% block (5% BSA, 1% fish gelatin) for 1 hour. The primary antibody (goat anti-clathrin light chain, Abcam, Cambridge, UK or rabbit anti-acetylated tubulin, Cell Signaling, Danvers, MA) was diluted 1:1000 in 20% block in PBS. Coverslips were incubated at 4º Celsius in a humidified chamber overnight. The primary antibody was removed and washed away with 3 10-minute PBS washes. The secondary (donkey anti-goat IgG-Alexafluor 488, Invitrogen, Carlsbad, CA or goat anti-rabbit IgG-Alexafluor 568, Invitrogen, Carlsbad, CA) was added and coverslips were incubated at room temperature for 1 hour. For cells stained with DAPI, DAPI (Biotium, Fremont, CA) was added for the last 10 minutes of secondary antibody incubation. This was followed by 3 more 10-minute PBS washes and finally mounting with Fluoromount-G. Cells were imaged using a Nikon widefield microscope. Z-stacks were obtained, and maximum intensity projections were created for visualization and sum slices were created for quantification using ImageJ.

Biotin ciliary isolation:
Procedure adapted from (W. Dentler 2013). 100mL of cells were grown in TAP for each condition until they reached an OD_{730} of 1.6 or above. Cells were then spun down and resuspended in M1 media and allowed to grow overnight. The next day cells were spun down at 1800rpm for 3 minutes and resuspended in HM Media (10mM HEPES, 5mM MgSO4, pH 7.2). Solid biotin (Thermo, Waltham, MA) was added to 20µg/mL for each strain and incubated for 5 minutes with agitation. Cells were diluted with 10 volumes of fresh M1 media before being spun down at 1800rpm for 3 minutes. After all cells were pelleted, they were washed with fresh M1 media three times. A pre sample was set aside (100mL) and the remainder of the cells were resuspended in 4.5 pH M1 media for 45 seconds before being spun down again at 1800rpm for 3 minutes. Cells were then resuspended in pH 7.0 media and allowed to regrow their cilia for 4 hours. A sample was taken pre-biotinylation to use as a control for non-specific streptavidin binding.

Meanwhile, the cilia were isolated from the pre sample. The samples were centrifuged for 3 minutes at 1800rpm. Supernatant was drained and each pellet was resuspended in 2 mL of 10mM HEPES (pH 7.4). This was repeated 2 times. Then each pellet was resuspended in 1 mL of fresh ice-cold 4% HMDS (10mM HEPES pH 7.4, 5mM MgSO4, 1mM DTT, 4% w/v sucrose). Cells were deciliated by incubating with 25mM dibucaine for 2 minutes. Then ice cold HMDS with 0.5mM EGTA was added (1mL per 1.5mL of cells). This was then centrifuged for 3 minutes at 1800rpm. Supernatant was collected for each sample. Then HMDS with 25% sucrose was layered beneath the supernatant (2 mL of 25% HMDS for 1mL of supernatant) to create an interface. This was centrifuged at 4º Celsius for 10 min at 2400rpm with no brake to avoid disrupting interface where cilia should now be located. Cilia were removed, pelleted at 21130xg for 30 minutes, then resuspended in lysis buffer (5% glycerol, 1% NP-40, 1mM DTT, 1X protease inhibitors). This was repeated with the post samples 4 hours following deciliation. An equal amount of protein was loaded to a 10% SDS-PAGE gel. The resulting gel was transferred to PVDF membrane. The membrane was washed 2x with PBSAT (PBST + 0.1% BSA), then incubated with HRP-conjugated streptavidin (Thermo, Waltham, MA) for 1 hour. The membrane was then washed 3 times with PBSAT (10 minutes each) and 3 times with PBST (15 minutes

each). Membrane was probed with West Pico Chemiluminescent Pico Substrate (Invitrogen, Carlsbad, CA). The same membrane was stripped of antibody and incubated with Coomassie Brilliant Blue to observe total protein.

Homology modeling and sequence studies:

Arp2/3 homology model was created using the Modeller plugin in UCSF Chimera. The template used was 1U2Z (Nolen, Littlefield, and Pollard 2004; Sali and Blundell 1993; Pettersen et al. 2004). Percent identity and similarity is calculated in relation to the human Arp2/3 complex members using a MUSCLE alignment in Geneious. The homology model was visualized and conservation was mapped on the protein surface using Chimera (Pettersen et al. 2004).

Statistical analysis:

Statistical analyses were done if GraphPad Prism Version 9. Superplots were created using the method in (Lord et al. 2020). For any experiments comparing 2 groups (**Figure 1B, 3D, 4C, 5C, and 5E**) an unpaired student's t-test was used to determine P value. For experiments comparing multiple samples at a single time point (**Figure 1A and 2B**), an ANOVA was used. Finally, for any graphs covering several time points (**Figure 1C, 1D, 2C, 3B, and 6E),** multiple comparisons were performed (Tukey's and Sidak's). For all experiments **** P<0.0001, *** P<0.001, ** P<0.01, * P<0.1.

ACKNOWLEDGEMENTS:

Our most sincere gratitude to William Dentler for providing his expertise especially in looking at the electron microscopy images and for his helpful advice, William Snell for generously providing the SAG1-HA strain, Masayuki Onishi for generously providing the *nap1* mutant strain, Henry Higgs for his feedback on version 1 of the manuscript, Ann Lavanway for assistance with microscopy, and the Avasthi lab for all their help throughout the project. We would also like to thank David Sept and Courtney M Schroeder for the help with the original version of this paper and for providing helpful comments throughout the process.

We also thank our funding sources including the Madison and Lila Self Graduate Fellowship at the University of Kansas Medical Center and the MIRA (R35GM128702). Finally, we thank the BioMT core at Dartmouth College (NIH/NIGMS COBRE award P20-GM113132), the Genomics and Molecular Biology Shared Resources Core (NCI Cancer Center Support Grant 5P30CA023108-37), and the KIDDRC NIH U54 HD 090216 at the University of Kansas Medical Center, Kansas City, KS 66160.

REFERENCES:

Adams, A E, and J R Pringle. 1984. "Relationship of Actin and Tubulin Distribution to Bud Growth in Wild-Type and Morphogenetic-Mutant Saccharomyces Cerevisiae." *Journal of Cell Biology* 98 (3): 934–45. https://doi.org/10.1083/jcb.98.3.934.

Aghamohammadzadeh, Soheil, and Kathryn R. Ayscough. 2009. "Differential Requirements for Actin during Yeast and Mammalian Endocytosis." *Nature Cell Biology* 11 (8): 1039–42. https://doi.org/10.1038/ncb1918.

Avasthi, Prachee, Masayuki Onishi, Joel Karpiak, Ryosuke Yamamoto, Luke Mackinder, Martin C Jonikas, Winfield S Sale, Brian Shoichet, John R Pringle, and Wallace F Marshall. 2014. "Actin Is Required for IFT Regulation in Chlamydomonas Reinhardtii." *Current Biology* 24 (17): 2025–32. https://doi.org/10.1016/j.cub.2014.07.038.

751 Ayscough, K. R., J. Stryker, N. Pokala, M. Sanders, P. Crews, and D. G. Drubin. 1997. "High Rates
752 of Actin Filament Turnover in Budding Yeast and Roles for Actin in Establishment and
753 Maintenance of Cell Polarity Revealed Using the Actin Inhibitor Latrunculin-A." *The*
754 *Journal of Cell Biology* 137 (2): 399–416. https://doi.org/10.1083/jcb.137.2.399.
755 Basu, Roshni, Emilia Laura Munteanu, and Fred Chang. 2014. "Role of Turgor Pressure in
756 Endocytosis in Fission Yeast." *Molecular Biology of the Cell* 25 (5): 679–87.
757 https://doi.org/10.1091/mbc.E13-10-0618.
758 Belzile, Olivier, Carmen I Hernandez-Lara, Qian Wang, and William J Snell. 2013. "Regulated
759 Membrane Protein Entry into Flagella Is Facilitated by Cytoplasmic Microtubules and
760 Does Not Require IFT." *Current Biology : CB* 23 (15): 1460–65.
761 https://doi.org/10.1016/j.cub.2013.06.025.
762 Bouck, G. Benjamin. 1971. "THE STRUCTURE, ORIGIN, ISOLATION, AND COMPOSITION OF THE
763 TUBULAR MASTIGONEMES OF THE OCHROMONAS FLAGELLUM." *Journal of Cell Biology*
764 50 (2): 362–84. https://doi.org/10.1083/jcb.50.2.362.
765 Campellone, K., and M. Welch. 2010. "A Nucleator Arms Race: Cellular Control of Actin
766 Assembly." *Nature Reviews Molecular Cell Biology* 11: 237–51.
767 Carlsson, Anders E., and Philip V. Bayly. 2014. "Force Generation by Endocytic Actin Patches in
768 Budding Yeast." *Biophysical Journal* 106 (8): 1596–1606.
769 https://doi.org/10.1016/j.bpj.2014.02.035.
770 Cheng, Xi, Gai Liu, Wenting Ke, Lijuan Zhao, Bo Lv, Xiaocui Ma, Nannan Xu, et al. 2017. "Building
771 a Multipurpose Insertional Mutant Library for Forward and Reverse Genetics in
772 Chlamydomonas." *Plant Methods* 13 (1): 36. https://doi.org/10.1186/s13007-017-0183-
773 5.
774 Craig, Evan W., David M. Mueller, Brae M. Bigge, Miroslava Schaffer, Benjamin D. Engel, and
775 Prachee Avasthi. 2019. "The Elusive Actin Cytoskeleton of a Green Alga Expressing Both
776 Conventional and Divergent Actins." *Molecular Biology of the Cell*, mbc.E19-03-0141.
777 https://doi.org/10.1091/mbc.E19-03-0141.
778 Dentler, W L, and C Adams. 1992. "Flagellar Microtubule Dynamics in Chlamydomonas:
779 Cytochalasin D Induces Periods of Microtubule Shortening and Elongation; and
780 Colchicine Induces Disassembly of the Distal, but Not Proximal, Half of the Flagellum."
781 *The Journal of Cell Biology* 117 (6): 1289–98. https://doi.org/10.1083/jcb.117.6.1289.
782 Dentler, William. 2013. "A Role for the Membrane in Regulating Chlamydomonas Flagellar
783 Length." *PLOS ONE* 8 (1): e53366. https://doi.org/10.1371/journal.pone.0053366.
784 Diener, Dennis R, Pietro Lupetti, and Joel L Rosenbaum. 2015. "Proteomic Analysis of Isolated
785 Ciliary Transition Zones Reveals the Presence of ESCRT Proteins." *Current Biology : CB* 25
786 (3): 379–84. https://doi.org/10.1016/j.cub.2014.11.066.
787 Farina, Francesca, Jérémie Gaillard, Christophe Guérin, Yohann Couté, James Sillibourne,
788 Laurent Blanchoin, and Manuel Théry. 2016. "The Centrosome Is an Actin-Organizing
789 Centre." *Nature Cell Biology* 18 (1): 65–75. https://doi.org/10.1038/ncb3285.
790 Goode, Bruce L, Julian A Eskin, and Beverly Wendland. 2015. "Actin and Endocytosis in Budding
791 Yeast." *Genetics* 199 (2): 315–58. https://doi.org/10.1534/genetics.112.145540.
792 Gournier, Helene, Erin D. Goley, Hanspeter Niederstrasser, Thong Trinh, and Matthew D.
793 Welch. 2001. "Reconstitution of Human Arp2/3 Complex Reveals Critical Roles of

794 Individual Subunits in Complex Structure and Activity." *Molecular Cell* 8 (5): 1041–52.
795 https://doi.org/10.1016/S1097-2765(01)00393-8.
796 Hetrick, Byron, Min Suk Han, Luke A Helgeson, and Brad J Nolen. 2013. "Small Molecules CK-666
797 and CK-869 Inhibit Actin-Related Protein 2/3 Complex by Blocking an Activating
798 Conformational Change." *Chemistry & Biology* 20 (5): 701–12.
799 https://doi.org/10.1016/j.chembiol.2013.03.019.
800 Hirono, Masafumi, Satomi Uryu, Akio Ohara, Takako Kato-Minoura, and Ritsu Kamiya. 2003.
801 "Expression of Conventional and Unconventional Actins in Chlamydomonas Reinhardtii
802 upon Deflagellation and Sexual Adhesion." *Eukaryotic Cell* 2 (3): 486–93.
803 https://doi.org/10.1128/ec.2.3.486-493.2003.
804 Inoue, Daisuke, Dorian Obino, Judith Pineau, Francesca Farina, Jérémie Gaillard, Christophe
805 Guerin, Laurent Blanchoin, Ana-Maria Lennon-Duménil, and Manuel Théry. 2019. "Actin
806 Filaments Regulate Microtubule Growth at the Centrosome." *The EMBO Journal* 38 (11).
807 https://doi.org/10.15252/embj.201899630.
808 Jack, Brittany, David M. Mueller, Ann C. Fee, Ashley L. Tetlow, and Prachee Avasthi. 2019.
809 "Partially Redundant Actin Genes in Chlamydomonas Control Transition Zone
810 Organization and Flagellum-Directed Traffic." *Cell Reports* 27 (8): 2459-2467.e3.
811 https://doi.org/10.1016/j.celrep.2019.04.087.
812 Jin, Hua, Susan Roehl White, Toshinobu Shida, Stefan Schulz, Mike Aguiar, Steven P. Gygi, J.
813 Fernando Bazan, and Maxence V. Nachury. 2010. "The Conserved Bardet-Biedl
814 Syndrome Proteins Assemble a Coat That Traffics Membrane Proteins to Cilia." *Cell* 141
815 (7): 1208–19. https://doi.org/10.1016/j.cell.2010.05.015.
816 Kaplan, Oktay I., David B. Doroquez, Sebiha Cevik, Rachel V. Bowie, Lara Clarke, Anna A.W.M.
817 Sanders, Katarzyna Kida, Joshua Z. Rappoport, Piali Sengupta, and Oliver E. Blacque.
818 2012. "Endocytosis Genes Facilitate Protein and Membrane Transport in C. Elegans
819 Sensory Cilia." *Current Biology* 22 (6): 451–60.
820 https://doi.org/10.1016/j.cub.2012.01.060.
821 Kato-Minoura, T, S Uryu, M Hirono, and R Kamiya. 1998. "Highly Divergent Actin Expressed in a
822 Chlamydomonas Mutant Lacking the Conventional Actin Gene." *Biochemical and*
823 *Biophysical Research Communications* 251 (1): 71–76.
824 https://doi.org/10.1006/bbrc.1998.9373.
825 Kiesel, Petra, Gonzalo Alvarez Viar, Nikolai Tsoy, Riccardo Maraspini, Peter Gorilak, Vladimir
826 Varga, Alf Honigmann, and Gaia Pigino. 2020. "The Molecular Structure of Mammalian
827 Primary Cilia Revealed by Cryo-Electron Tomography." *Nature Structural & Molecular*
828 *Biology*, September. https://doi.org/10.1038/s41594-020-0507-4.
829 Kim, Joon, Ji Eun Lee, Susanne Heynen-Genel, Eigo Suyama, Keiichiro Ono, Kiyoung Lee, Trey
830 Ideker, Pedro Aza-Blanc, and Joseph G. Gleeson. 2010. "Functional Genomic Screen for
831 Modulators of Ciliogenesis and Cilium Length." *Nature* 464 (7291): 1048–51.
832 https://doi.org/10.1038/nature08895.
833 Langousis, Gerasimos, Michelle M. Shimogawa, Edwin A. Saada, Ajay A. Vashisht, Roberto
834 Spreafico, Andrew R. Nager, William D. Barshop, Maxence V. Nachury, James A.
835 Wohlschlegel, and Kent L. Hill. 2016. "Loss of the BBSome Perturbs Endocytic Trafficking
836 and Disrupts Virulence of Trypanosoma Brucei." *Proceedings of the National Academy*

of Sciences of the United States of America 113 (3): 632–37. https://doi.org/10.1073/pnas.1518079113.

Lefebvre, P. A., S. A. Nordstrom, J. E. Moulder, and J. L. Rosenbaum. 1978. "Flagellar Elongation and Shortening in Chlamydomonas. IV. Effects of Flagellar Detachment, Regeneration, and Resorption on the Induction of Flagellar Protein Synthesis." *The Journal of Cell Biology* 78 (1): 8–27. https://doi.org/10.1083/jcb.78.1.8.

Lefebvre, Paul A. 1995. "Flagellar Amputation and Regeneration in Chlamydomonas." In *Methods in Cell Biology*, 47:3–7. Elsevier.

Li, Xiaobo, Weronika Patena, Friedrich Fauser, Robert E. Jinkerson, Shai Saroussi, Moritz T. Meyer, Nina Ivanova, et al. 2019. "A Genome-Wide Algal Mutant Library and Functional Screen Identifies Genes Required for Eukaryotic Photosynthesis." *Nature Genetics* 51 (4): 627–35. https://doi.org/10.1038/s41588-019-0370-6.

Loeffelholz, Ottilie von, Andrew Purkiss, Luyan Cao, Svend Kjaer, Naoko Kogata, Guillaume Romet-Lemonne, Michael Way, and Carolyn A. Moores. 2020. "Cryo-EM of Human Arp2/3 Complexes Provides Structural Insights into Actin Nucleation Modulation by ARPC5 Isoforms." *BioRxiv*, January, 2020.05.01.071704. https://doi.org/10.1101/2020.05.01.071704.

Lord, Samuel J., Katrina B. Velle, R. Dyche Mullins, and Lillian K. Fritz-Laylin. 2020. "SuperPlots: Communicating Reproducibility and Variability in Cell Biology." *The Journal of Cell Biology* 219 (6). https://doi.org/10.1083/jcb.202001064.

Milenkovic, Ljiljana, Matthew P. Scott, and Rajat Rohatgi. 2009. "Lateral Transport of Smoothened from the Plasma Membrane to the Membrane of the Cilium." *The Journal of Cell Biology* 187 (3): 365–74. https://doi.org/10.1083/jcb.200907126.

Molla-Herman, Anahi, Rania Ghossoub, Thierry Blisnick, Alice Meunier, Catherine Serres, Flora Silbermann, Chris Emmerson, et al. 2010. "The Ciliary Pocket: An Endocytic Membrane Domain at the Base of Primary and Motile Cilia." *Journal of Cell Science* 123 (Pt 10): 1785–95. https://doi.org/10.1242/jcs.059519.

Nachury, Maxence V., Alexander V. Loktev, Qihong Zhang, Christopher J. Westlake, Johan Peränen, Andreas Merdes, Diane C. Slusarski, et al. 2007. "A Core Complex of BBS Proteins Cooperates with the GTPase Rab8 to Promote Ciliary Membrane Biogenesis." *Cell* 129 (6): 1201–13. https://doi.org/10.1016/j.cell.2007.03.053.

Nachury, Maxence V., E. Scott Seeley, and Hua Jin. 2010. "Trafficking to the Ciliary Membrane: How to Get across the Periciliary Diffusion Barrier?" *Annual Review of Cell and Developmental Biology* 26: 59–87. https://doi.org/10.1146/annurev.cellbio.042308.113337.

Nolen, Brad J., Ryan S. Littlefield, and Thomas D. Pollard. 2004. "Crystal Structures of Actin-Related Protein 2/3 Complex with Bound ATP or ADP." *Proceedings of the National Academy of Sciences of the United States of America* 101 (44): 15627. https://doi.org/10.1073/pnas.0407149101.

Onishi, M., K. Pecani, T. th Jones, J. R. Pringle, and F. R. Cross. 2018. "F-Actin Homeostasis through Transcriptional Regulation and Proteasome-Mediated Proteolysis." *Proc Natl Acad Sci U S A* 115 (28): E6487-e6496. https://doi.org/10.1073/pnas.1721935115.

Onishi, M., J. R. Pringle, and F. R. Cross. 2016. "Evidence That an Unconventional Actin Can Provide Essential F-Actin Function and That a Surveillance System Monitors F-Actin

Integrity in Chlamydomonas." *Genetics* 202 (3): 977–96. https://doi.org/10.1534/genetics.115.184663.

Onishi, Masayuki, James G. Umen, Frederick R. Cross, and John R. Pringle. 2019. "Cleavage-Furrow Formation without F-Actin in Chlamydomonas</Em>." *BioRxiv*, January, 789016. https://doi.org/10.1101/789016.

Papermaster, D. S., B. G. Schneider, and J. C. Besharse. 1985. "Vesicular Transport of Newly Synthesized Opsin from the Golgi Apparatus toward the Rod Outer Segment. Ultrastructural Immunocytochemical and Autoradiographic Evidence in Xenopus Retinas." *Investigative Ophthalmology & Visual Science* 26 (10): 1386–1404.

Park, Tae Joo, Brian J. Mitchell, Philip B. Abitua, Chris Kintner, and John B. Wallingford. 2008. "Dishevelled Controls Apical Docking and Planar Polarization of Basal Bodies in Ciliated Epithelial Cells." *Nature Genetics* 40 (7): 871–79. https://doi.org/10.1038/ng.104.

Pasquale, S M, and U W Goodenough. 1987. "Cyclic AMP Functions as a Primary Sexual Signal in Gametes of Chlamydomonas Reinhardtii." *The Journal of Cell Biology* 105 (5): 2279–92. https://doi.org/10.1083/jcb.105.5.2279.

Pedersen, Lotte B., and Joel L. Rosenbaum. 2008. "Intraflagellar Transport (IFT) Role in Ciliary Assembly, Resorption and Signalling." *Current Topics in Developmental Biology* 85: 23–61. https://doi.org/10.1016/S0070-2153(08)00802-8.

Pettersen, Eric F., Thomas D. Goddard, Conrad C. Huang, Gregory S. Couch, Daniel M. Greenblatt, Elaine C. Meng, and Thomas E. Ferrin. 2004. "UCSF Chimera--a Visualization System for Exploratory Research and Analysis." *Journal of Computational Chemistry* 25 (13): 1605–12. https://doi.org/10.1002/jcc.20084.

Robinson, Robert C., Kirsi Turbedsky, Donald A. Kaiser, Jean-Baptiste Marchand, Henry N. Higgs, Senyon Choe, and Thomas D. Pollard. 2001. "Crystal Structure of Arp2/3 Complex." *Science* 294 (5547): 1679. https://doi.org/10.1126/science.1066333.

Rohatgi, Rajat, and William J Snell. 2010. "The Ciliary Membrane." *Current Opinion in Cell Biology* 22 (4): 541–46. https://doi.org/10.1016/j.ceb.2010.03.010.

Rosenbaum, J. L., J. E. Moulder, and D. L. Ringo. 1969. "Flagellar Elongation and Shortening in Chlamydomonas. The Use of Cycloheximide and Colchicine to Study the Synthesis and Assembly of Flagellar Proteins." *The Journal of Cell Biology* 41 (2): 600–619. https://doi.org/10.1083/jcb.41.2.600.

Saito, Masaki, Wataru Otsu, Kuo-Shun Hsu, Jen-Zen Chuang, Teruyuki Yanagisawa, Vincent Shieh, Taku Kaitsuka, Fan-Yan Wei, Kazuhito Tomizawa, and Ching-Hwa Sung. 2017. "Tctex-1 Controls Ciliary Resorption by Regulating Branched Actin Polymerization and Endocytosis." *EMBO Reports* 18 (8): 1460–72. https://doi.org/10.15252/embr.201744204.

Sali, A., and T. L. Blundell. 1993. "Comparative Protein Modelling by Satisfaction of Spatial Restraints." *Journal of Molecular Biology* 234 (3): 779–815. https://doi.org/10.1006/jmbi.1993.1626.

Spector, Ilan, Nava R. Shochet, Dina Blasberger, and Yoel Kashman. 1989. "Latrunculins—Novel Marine Macrolides That Disrupt Microfilament Organization and Affect Cell Growth: I. Comparison with Cytochalasin D." *Cell Motility* 13 (3): 127–44. https://doi.org/10.1002/cm.970130302.

924 Wingfield, Jenna L, Ilaria Mengoni, Heather Bomberger, Yu-Yang Jiang, Jonathon D Walsh, Jason
925 M Brown, Tyler Picariello, et al. 2017. “IFT Trains in Different Stages of Assembly Queue
926 at the Ciliary Base for Consecutive Release into the Cilium.” Edited by Erwin J G
927 Peterman. *ELife* 6 (May): e26609. https://doi.org/10.7554/eLife.26609.
928 Winter, D. C., E. Y. Choe, and R. Li. 1999. “Genetic Dissection of the Budding Yeast Arp2/3
929 Complex: A Comparison of the in Vivo and Structural Roles of Individual Subunits.”
930 *Proceedings of the National Academy of Sciences of the United States of America* 96
931 (13): 7288–93. https://doi.org/10.1073/pnas.96.13.7288.
932 Wood, Christopher R., and Joel L. Rosenbaum. 2014. “Proteins of the Ciliary Axoneme Are
933 Found on Cytoplasmic Membrane Vesicles during Growth of Cilia.” *Current Biology* 24
934 (10): 1114–20. https://doi.org/10.1016/j.cub.2014.03.047.
935 Wu, Chien-Ting, Hsin-Yi Chen, and Tang K. Tang. 2018. “Myosin-Va Is Required for Preciliary
936 Vesicle Transportation to the Mother Centriole during Ciliogenesis.” *Nature Cell Biology*
937 20 (2): 175–85. https://doi.org/10.1038/s41556-017-0018-7.
938 Zuo, Xiaofeng, Wei Guo, and Joshua H. Lipschutz. 2009. “The Exocyst Protein Sec10 Is Necessary
939 for Primary Ciliogenesis and Cystogenesis In Vitro.” *Molecular Biology of the Cell* 20 (10):
940 2522–29. https://doi.org/10.1091/mbc.e08-07-0772.
941